

Coherent-feedback-induced photon blockade and optical bistability by an optomechanical controller

Yu-Long Liu,¹ Zhong-Peng Liu,² Jing Zhang,^{2,3} and Yu-xi Liu^{1,3,*}

¹*Institute of Microelectronics, Tsinghua University, Beijing 100084, China*

²*Department of Automation, Tsinghua University, Beijing 100084, China*

³*Tsinghua National Laboratory for Information Science and Technology (TNList), Beijing 100084, China*

(Dated: July 14, 2014)

It is well-known that some nonlinear phenomena such as strong photon blockade are hard to be observed in optomechanical system with current experimental technology. Here, we present a coherent feedback control strategy in which a linear cavity is coherently controlled by an optomechanical controller in a feedback manner. The coherent feedback loop transfers and enhances quantum non-linearity from the controller to the controlled cavity, which makes it possible to observe strong nonlinear effects in either linear cavity or optomechanical cavity. More interestingly, we find that the strong photon blockade under single-photon optomechanical weak coupling condition could be observed in the quantum regime. Additionally, the coherent feedback loop leads to two-photon and multiphoton tunnelings for the controlled linear cavity, which are also typical quantum nonlinear phenomenon. We hope that our work can give new perspectives in engineering nonlinear quantum phenomena.

PACS numbers: 42.65.Es, 42.65.Ky, 75.30.Cr

I. INTRODUCTION

Similar to Coulomb blockade for electrons in mesoscopic electronic devices [1–3], photon blockade [4, 5] is a typical nonlinear quantum optical effect, where the subsequent photons are prevented from resonantly entering the cavity due to the strong nonlinear photon-photon interaction. This phenomenon can be observed by the so-called photon antibunching in photon correlation measurements. The nonlinear photon-photon interaction at single-photon level is inherently nonclassical and provides a way to control signal photon via photonic devices, which is essential to various emerging techniques, such as single-photon transistor [6], photon routing [7–11], generation of non-classical light [12], quantum information processing with photonic qubits [13–15], optical communication [16], and optical quantum computer [17]. The photon blockade has been experimentally demonstrated in, e.g., cavity-QED systems with the strong atom-cavity coupling [18], a quantum dot strongly coupled to a photonic crystal resonator [19], and circuit-QED systems [20, 21]. It is generally recognized that the nonlinear photon coupling strength should be far larger than the cavity decay rate when the single-photon blockade occurs. Thus engineering nonlinear photon-photon coupling is an important task for single-photon devices.

Recently, cavity optomechanics becomes a rapidly growing field of research, in which nonlinear couplings between the electromagnetic and mechanical degrees of freedom [22–26] lead to various interesting phenomena. The nonlinear optomechanical coupling can be applied to the detection of gravitational waves [27–29], the ob-

servation of quantum effects in the mesoscopic and macroscopic scales [30]. The optomechanical system can also be used to build sensitive mass, force and displacement detectors [31], and the hardware for realizing quantum information processing [32]. Various achievements have been made both theoretically and experimentally in optomechanical systems, for instance, the cooling of the mechanical resonator to its ground state, which paves the way to study the physical effects on the boundary between classical and quantum mechanics [33–47], the mechanical oscillations induced by the radiation pressure [48, 49], electromagnetically induced transparency [50–54], entanglement between optical and mechanical modes [55, 56], optomechanical transducers [57], normal mode splitting [58], and coherent optical wavelength conversion [59–65]. Especially, the nonlinear Kerr effect can also be realized in optomechanical systems [66–68], which can be used to engineer nonlinear photon-photon interaction. Thus, the optomechanical systems might also be very important candidates to act as single-photon devices, e.g., a single-photon router [69].

It has been theoretically shown that the single-photon phenomena and photon blockade can be realized in optomechanical systems [70–74] when the single-photon optomechanical coupling strength is much larger than the cavity decay rate. However, in current experimental technology, the optomechanical-coupling induced Kerr nonlinearity is not strong enough to be used for observing such single-photon effect. Several approaches have been proposed for enhancing the photon-photon interaction using coupled optomechanical systems [75, 76]. However, the strong single-photon optomechanical coupling is still a necessary condition for the demonstration of photon blockade. Recent studies showed [77] that particular nonlinear effects are hopeful to be observed in a linear cavity, which is coupled to an optomechanical sys-

*Electronic address: yuxiliu@mail.tsinghua.edu.cn

tem with the weak optomechanical coupling. However, photon blockade is still hard to be observed in optomechanical system. Moreover, this method requires strong coupling between the linear cavity and the optomechanical cavity via spatial proximity. However, individual addressability of each cavity is still an arduous challenge in current experimental technology [78].

We recently study a method to induce nonlinearity into a linear cavity by coherent feedback control using a circuit QED system as a controller [79, 80]. Motivated by studies [66–77] and considering progress on quantum coherent feedback methods [81–93], we propose an approach to realize an optomechanically-based single-photon device by replacing the circuit QED system in the coherent feedback approach [80] with a traditional optomechanical system. Such a coherent-feedback strategy can liberate both the linear cavity and the optomechanical system in space and eliminate the slashing requirement on individual addressability or large coupling strength between linear cavity and optomechanical cavity. Moreover, we find that photon blockade phenomenon can be observed even in the weak optomechanical coupling regime for such a design. We will also show that the damping effects of the controlled cavity and the optomechanical controller are actually crucial for achieving photon blockade in such coherent-feedback approach. This is different from other existing photon blockade systems in which the cavity loss always plays a negative role.

In our approach, the output of the controlled cavity is unitarily processed by optomechanical controller, and then the processed output field is fed into the controlled cavity again. Such a coherent-feedback strategy preserves the quantum coherence of the system and also reduces the feedback-induced time delay. In contrast to direct coherent feedback [82], we use field-mediated coherent feedback [85–87] method, in which the information flow is uniquely determined by the propagation direction of the quantum field and thus it is easier to be realized in experiments.

The paper is organized as follows. In Sec. II, we briefly summarize the main results of quantum input-output and coherent feedback control theory which are related to our study. In Sec. III, we present the mathematical descriptions of our feedback control system, i.e., a linear cavity coupled to an optomechanical system in the feedback configuration. We introduce both the steady-state equations and the quantum Langevin equations with quantum and thermal fluctuations to model the dynamics of our feedback control system. In Sec. IV, we study the nonlinear effects of the controlled linear cavity induced by the optomechanical system in the semi-classical regime. The nonlinear effects of the controlled cavity, such as optical bistability, are induced by the nonlinear dissipative coupling between the controlled system and the intermediate quantum field. In Sec. V, we studied the statistical properties of photons in both the optomechanical controller and the controlled cavity with two different driving methods in the quantum regime. Our re-

sults show that the strong photon blockade effect can be observed even in the weak single-photon optomechanical coupling regime. Feedback-induced photon tunneling processes, especially two- and three-photon tunnelings, are also discussed. Conclusions and perspective discussions are given in Sec. VI.

II. FIELD-MEDIATED COHERENT FEEDBACK

The quantum system with an input field a_{in} and an output field a_{out} can be schematically shown in Fig. 1. The input field a_{in} can be described by a continuum of harmonic oscillators. Under the Markovian approximation, the Hamiltonian H of the whole system can be given as [94]

$$H = H_{\text{sys}} + i[a_{\text{in}}^\dagger L - L^\dagger a_{\text{in}}]. \quad (1)$$

Here, we assume $\hbar = 1$. We also use H_{sys} to denote the Hamiltonian of the quantum system. $L = \sqrt{\gamma}a$ is the Lindblad operator induced from the system and the bath field, where a (a^\dagger) is the annihilation (creation) operator of the system. The input field a_{in} is defined as

$$a_{\text{in}} = \frac{1}{\sqrt{2\pi}} \int_{-\infty}^{+\infty} b(\omega) e^{-i\omega t} d\omega. \quad (2)$$

where $b(\omega)$ ($b^\dagger(\omega)$) is the annihilation (creation) operator of the bath mode with frequency ω satisfying $[b(\omega), b^\dagger(\omega')] = \delta(\omega - \omega')$ and $[b(\omega), b(\omega')] = 0$.

The system shown in Fig. 1 can also be modelled by a set of parameters $G = (S, L, H)$ [86]. Here, S denotes the scattering matrix, H and L are given in Eq. (1). The (S, L, H) notation can be used conveniently to study the networks of coupled open quantum systems for quantum control analysis and design.

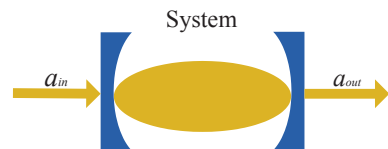


FIG. 1: (Color online) Schematic diagram of a single quantum system with the input field a_{in} and output field a_{out} .

The theory of the single quantum system with input and output fields, as shown in Fig. 1, can be generalized to a Markovian quantum cascaded system as shown in Fig. 2(a). We assume that the output field of the first system, described by $G_1 = (S_1, L_1, H_1)$, acts as the input field of the second system, described by $G_2 = (S_2, L_2, H_2)$. This coupled cascade system is equivalent to the system, described by [86]

$$G = (S_{\text{eff}}, H_{\text{eff}}, L_{\text{eff}}), \quad (3)$$

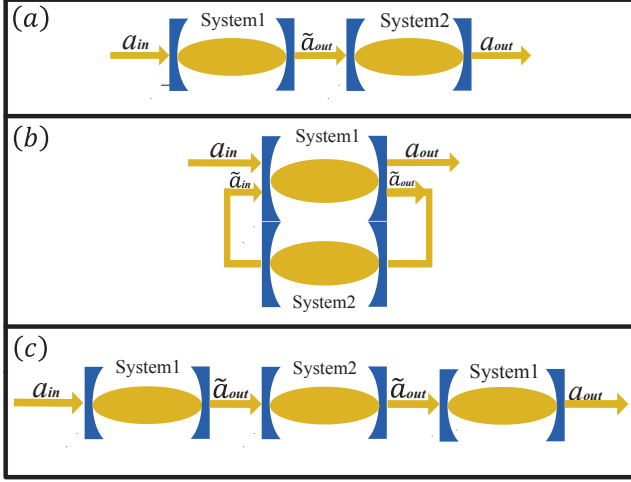


FIG. 2: (Color online) Schematic diagrams of the cascade quantum system. (a) Cascade system with two cascaded-connected components, in which the output of the first system acts as the input field of the second system. (b) Proposed coherent feedback system, in which the output of the first system is fed into the quantum controller coherently and then the output of the quantum controller is coherently fed back to act as the input of the first system. (c) Equivalent schematic of coherent feedback system, which can be seen as the controlled system cascaded-connected with the controller system and then cascaded-connected with itself.

with

$$S_{\text{eff}} = S_2 S_1, \quad L_{\text{eff}} = L_2 + S_2 L_1, \quad (4)$$

$$H_{\text{eff}} = H_1 + H_2 + \frac{1}{2i} (L_2^\dagger S_2 L_1 - L_1^\dagger S_2^\dagger L_2). \quad (5)$$

As shown in Fig. 2(b), we now focus on another scenario in which the output of the first system $G_1 = (S_1, L_1, H_1)$ is taken as the input of the second system with $G_2 = (S_2, L_2, H_2)$, and simultaneously the output of the second system is taken as the input of the first system, by which a coherent-feedback loop is constructed. In Fig. 2, both the scattering matrices of these two components are identity matrix I , that is, $S_1 = S_2 = S = I$. Such coherent-feedback system is equivalent to a system in which $G_1 = (I, L_1, H_1)$ is first cascaded-connected to $G_2 = (I, L_2, H_2)$ and then cascade-connected to $G_3 = (I, L_3, H_1)$ as shown in Fig. 2(c). The whole feedback system, shown in both Fig. 2(b) and Fig. 2(c), can be described by

$$(\tilde{S}, \tilde{L}, \tilde{H}), \quad (6)$$

with

$$\tilde{S} = S, \quad \tilde{L} = L_1 + L_2 + L_3, \quad (7)$$

$$\tilde{H} = H_1 + H_2 + \frac{1}{2i} \left[(L_2^\dagger L_1 + L_3^\dagger L_2 + L_3^\dagger L_1) - \text{H.C.} \right]. \quad (8)$$

III. MODEL AND HAMILTONIAN

As schematically shown in Fig. 3, we study a linear cavity which is controlled by a standard optomechanical system. The output field of the controlled cavity is coherently fed into the optomechanical controller and then fed back into the controlled cavity again. The controlled cavity can be taken as a transmission line resonator, a toroidal microresonator, a cavity with two mirrors, or a defect cavity in photonic crystal. Without loss of generality and for simplicity, we will focus on the cavity with two mirrors which can support two input channels and two output channels. The dissipation of the controlled

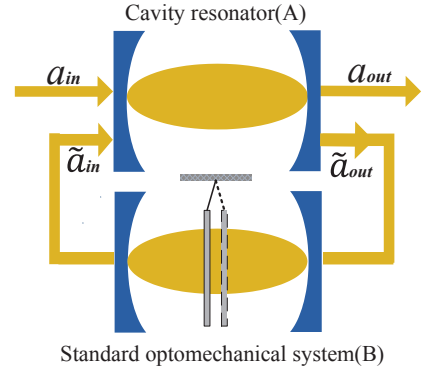


FIG. 3: (Color online) Schematic diagrams for a cavity (A) coherently feedback controlled by a standard optomechanical system (B).

cavity via the vacuum fluctuation field a_{in} is described by the Lindblad operator $L_a = \sqrt{\kappa}a$. a (a^\dagger) is the annihilation (creation) operator of the controlled cavity with the decay rate κ and the frequency ω_s . $H_a = \omega_s a^\dagger a$ describes the Hamiltonian of the controlled cavity. With the (S, L, H) notation, the controlled cavity can be described by (S, L_a, H_a) . The output of the controlled cavity is fed into a standard optomechanical system, which serves as a controller to induce and manipulate the nonlinearity of the controlled cavity. The resonant frequency of the cavity of optomechanical system is modulated by the position of a mechanical resonator. A monochromatic coherent light field with the frequency ω_d and amplitude ϵ is used to drive the cavity of the optomechanical system. The driven Hamiltonian H_c of the optomechanical system is given by

$$H_c = \omega_c c^\dagger c + \omega_m b^\dagger b + g_0 c^\dagger c (b^\dagger + b) + \epsilon (c^\dagger e^{i\omega_d t} + c e^{-i\omega_d t}), \quad (9)$$

where c (c^\dagger) is the annihilation (creation) operator of the optomechanical cavity, b (b^\dagger) is the annihilation (creation) operator of the mechanical model with frequency ω_m . The parameter g_0 is the single-photon optomechanical coupling strength. The optomechanical controller interacts with the intermediate field via the dissipation channel of the cavity field described by the Lindblad op-

erator $L_c = \sqrt{\gamma}c$. Afterward, the output of the controller is fed into the controlled system via the dissipation channel $L_f = \sqrt{\kappa_f}a$ to complete the whole coherent feedback loop. With the (S, L, H) notation, the optomechanical controller can be described by $(S, \sqrt{\gamma}c, H_c)$.

The whole coherent feedback system can be described by three cascaded-connected subsystems which have been schematically shown in Fig. 2(b). Thus, the cascade system, with the first ($G_1 = (I, \sqrt{\kappa}a, \omega_s a^\dagger a)$), the second ($G_2 = (I, \sqrt{\gamma}c, H_c)$), and, the third ($G_3 = (I, \sqrt{\kappa_f}a, \omega_s a^\dagger a)$) subsystems, can be described by

$$(S', L', H').$$

with

$$S' = I, L' = \sqrt{\kappa}a + \sqrt{\gamma}c + \sqrt{\kappa_f}a, \quad (10)$$

$$H' = H_a + H_c + \frac{i}{2}(\sqrt{\gamma\kappa} - \sqrt{\gamma\kappa_f})(a^\dagger c - c^\dagger a). \quad (11)$$

In the rotating reference frame with unitary transformation $R(t) = \exp[i\omega_d(c^\dagger c + a^\dagger a)t]$, the Hamiltonian in Eq. (11) becomes

$$\begin{aligned} \tilde{H} = & \Delta_s a^\dagger a + \Delta_c c^\dagger c + \omega_m b^\dagger b + g_0 c^\dagger c(b^\dagger + b) \\ & + \epsilon(c^\dagger + c) + \frac{i}{2}(\sqrt{\gamma\kappa} - \sqrt{\gamma\kappa_f})(a^\dagger c - c^\dagger a), \end{aligned} \quad (12)$$

where $\Delta_s = \omega_s - \omega_d$ and $\Delta_c = \omega_c - \omega_d$ are the detuning frequencies.

Using the input-output theory, the dynamics of the whole system is described by the quantum Langevin equation (QLEs) [79, 80, 93]

$$\begin{aligned} \dot{a} = & -i\Delta_s a - \frac{1}{2}(\sqrt{\kappa} + \sqrt{\kappa_f})^2 a - \sqrt{\gamma\kappa_f}c \\ & - (\sqrt{\kappa} + \sqrt{\kappa_f})a_{\text{in}}, \end{aligned} \quad (13)$$

$$\dot{b} = -i\omega_m b - ig_0 c^\dagger c - \frac{\gamma_m}{2}b - \sqrt{\gamma_m}b_{\text{in}}, \quad (14)$$

$$\begin{aligned} \dot{c} = & -i\Delta_c c - ig_0 c(b^\dagger + b) - \sqrt{\kappa\gamma}a - \frac{1}{2}\gamma c \\ & - i\epsilon - \sqrt{\gamma}a_{\text{in}}, \end{aligned} \quad (15)$$

where γ_m is the damping rate of the mechanical resonator. b_{in} denotes the thermal noise acting on the mechanical resonator which satisfies the Markovian correlation relation

$$\langle b_{\text{in}}(t)b_{\text{in}}^\dagger(t') \rangle = (n_{\text{th}} + 1)\delta(t - t'), \quad (16)$$

The mean thermal occupation number of b_{in} can be calculated by $n_{\text{th}} = [\exp(\omega_m/k_B T) - 1]^{-1}$. We also assume that the vacuum fluctuation a_{in} satisfies

$$\langle a_{\text{in}}(t)a_{\text{in}}^\dagger(t') \rangle = \delta(t - t'). \quad (17)$$

where the frequency of the controlled cavity is assumed to be much higher than that of the mechanical resonator,

thus the temperature effect on the cavity field has been neglected.

Using the mean field approximation, the time evolutions of the mean values of each operator can be given as:

$$\begin{aligned} \frac{d\langle a \rangle}{dt} = & -i\Delta_s \langle a \rangle - \frac{1}{2}(\sqrt{\kappa} + \sqrt{\kappa_f})^2 \langle a \rangle \\ & - \sqrt{\gamma\kappa_f} \langle c \rangle, \end{aligned} \quad (18)$$

$$\frac{d\langle b \rangle}{dt} = -i\omega_m \langle b \rangle - ig_0 |c|^2 - \frac{\gamma_m}{2} \langle b \rangle, \quad (19)$$

$$\begin{aligned} \frac{d\langle c \rangle}{dt} = & -i\Delta_c \langle c \rangle - ig_0 \langle c \rangle (\langle b \rangle^* + \langle b \rangle) - i\epsilon \\ & - \sqrt{\kappa\gamma} \langle a \rangle - \frac{1}{2}\gamma \langle c \rangle. \end{aligned} \quad (20)$$

IV. COHERENT FEEDBACK INDUCED OPTICAL BISTABILITY

It is known that the bistability can be found in the standard optomechanical system [67]. Let us now first study how the optical nonlinear behavior in the controlled linear cavity can be induced by a standard optomechanical system using coherent feedback method. In other words, we study how the optical nonlinearity in optomechanical system can be manipulated and transferred to a linear cavity by using coherent feedback. By solving Eqs. (18-20) with $\langle \dot{a} \rangle_s = \langle \dot{b} \rangle_s = \langle \dot{c} \rangle_s = 0$, we can obtain the steady-state values

$$A_0 = \frac{-\sqrt{\gamma\kappa_f}}{[i\Delta_s + \frac{1}{2}(\sqrt{\kappa} + \sqrt{\kappa_f})^2]} C_0, \quad (21)$$

$$B_0 = \frac{-ig_0}{i\omega_m + \frac{\gamma_m}{2}} |C_0|^2, \quad (22)$$

$$C_0 = \frac{-i\epsilon - \sqrt{\kappa\gamma}A_0}{i\Delta_c + ig_0(B_0^* + B_0) + \frac{1}{2}\gamma}, \quad (23)$$

of the cavity fields and mechanical resonator. Here, $A_0 = \langle a \rangle_s$, $B_0 = \langle b \rangle_s$, and $C_0 = \langle c \rangle_s$ denote the steady state values of the average $\langle a \rangle$, $\langle b \rangle$ and $\langle c \rangle$.

Using Eqs. (21-23), we can obtain a third-order polynomial root equation for the normalized mean photon number in the cavity of the optomechanical system

$$f(\lambda) = 4\lambda^3 - 4y\lambda^2 + (x^2 + y^2)\lambda - z = 0. \quad (24)$$

Compare Eq. (24) with that in Ref. [67], we find that Eq. (24) has the same form as that in Ref. [67] when $x = 0.5$. Moreover, the coefficient y has also been changed by the feedback control. Here, we have used the condition $Q_m = \omega_m/\gamma_m \gg 1$ and introduced several dimensionless parameters

$$\begin{aligned} x = & \frac{p_1}{\gamma}, \quad y = \frac{p_2}{\gamma}, \quad z = k \frac{|\epsilon|^2}{\gamma^2}, \\ k = & \frac{g_0^2}{\gamma\omega_m}, \quad \lambda = kn, \quad n = |C_0|^2, \end{aligned} \quad (25)$$

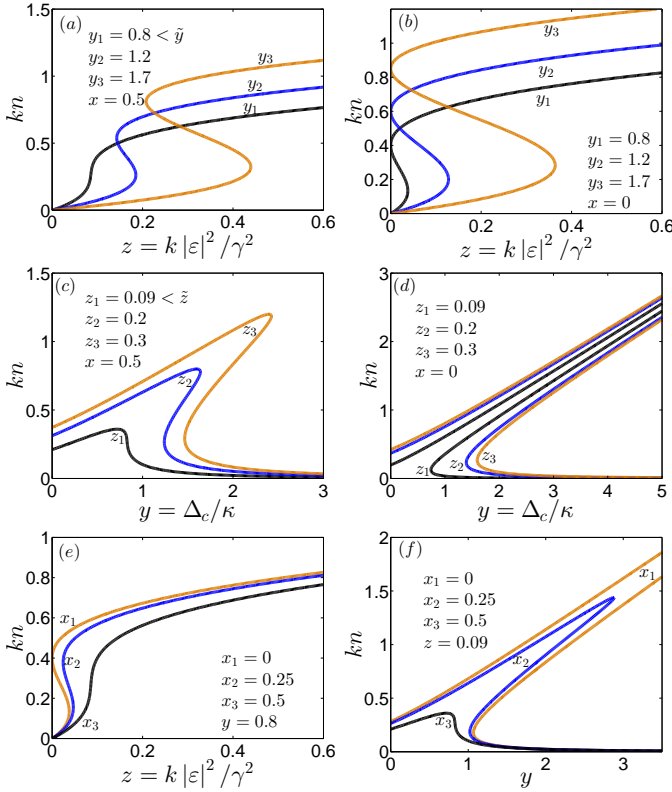


FIG. 4: (Color online) Optical bistability in the semiclassical regime. Typical curves for the mean-field cavity occupation kn as a function of the dimensionless driving power z (a,b), the detuning parameter y (c,d) and the detuning parameter x (e,f). We show the mean-field occupation kn as a function of driving power z for fixed detuning y and the detuning parameter x of cavity A was set to 0.5 in (a) and 0 in (b). We show the mean-field occupation kn as a function of detuning y for fixed driving power z . The detuning parameter x was set to 0.5 in (c) and 0 in (d). We also show the mean-field occupation kn as a function of driving power z for fixed detuning y and detuning parameter $x_1 = 0, x_2 = 0.25, x_3 = 0.5$ in (e), and kn as a function of detuning parameter y for fixed driving power z and detuning parameter $x_1 = 0, x_2 = 0.25, x_3 = 0.5$ in (f).

with

$$p_2 = \Delta_c + \frac{4\gamma\sqrt{\kappa\kappa_f}\Delta_s}{[4\Delta_s^2 + (\sqrt{\kappa} + \sqrt{\kappa_f})^4]}, \quad (26)$$

$$p_1 = \frac{\gamma}{2} - \frac{2\gamma\sqrt{\kappa\kappa_f}(\sqrt{\kappa} + \sqrt{\kappa_f})^2}{[4\Delta_s^2 + (\sqrt{\kappa} + \sqrt{\kappa_f})^4]}. \quad (27)$$

It can be found that k characterizes the optical nonlinearity induced by the mechanical resonator, and the parameters x and y are determined by the detuning frequencies Δ_c and Δ_s when all of decay rates are fixed. z is called the normalized power of the driving field and n is the mean photon number inside the cavity of the optomechanical system.

We can also find that the mean photon number $n_A =$

$|A_0|^2$ of the controlled cavity can be given by

$$n_A = Kn, \quad (28)$$

with

$$K = \frac{4\gamma\kappa_f}{4\Delta_s^2 + (\sqrt{\kappa} + \sqrt{\kappa_f})^4}, \quad (29)$$

which shows that the mean photon number n_A of the controlled cavity is proportional to the mean photon number n of the controller cavity. Without loss of generality, we assume that $K = 1$ for the following discussions such that both n_A and n simply satisfy Eq. (24), which can have either one or three roots, depending on the dimensionless parameters x , y and z .

In fact, when Eq. (24) is solved, three real roots can be found only if: (i) the parameters y and z are larger than threshold values \tilde{y} and \tilde{z} for given parameter x , that is,

$$y > \tilde{y} = \sqrt{3}x, \quad (30)$$

$$z > \tilde{z} = \frac{4}{27}\tilde{y}^3, \quad (31)$$

and (ii) the parameter z must be in the region $z_-(y) < z < z_+(y)$ with

$$z_{\pm}(y) = \frac{1}{27}[y(y^2 + 3\tilde{y}^2) \pm (y^2 - \tilde{y}^2)^{3/2}]. \quad (32)$$

The first externally controllable parameter, that can be used to control the bistability behavior, is the normalized driving power z . In Fig. 4(a), we show the normalized mean photon number kn as a function of z for $x = 0.5$, corresponding to the threshold value $\tilde{y} = \sqrt{3}/2$, and three different parameters $y_1 = 0.8 < \sqrt{3}/2$, $y_2 = 1.2 > \sqrt{3}/2$ and $y_3 = 1.7 > \sqrt{3}/2$, respectively. Fig. 4(a) clearly shows that the optical bistability cannot be observed when $y_1 < \sqrt{3}/2$ in contrast that the bistability can be observed when $y_2, y_3 > \sqrt{3}/2$. From Eq. (30) and Eq. (26), we can find that the threshold value \tilde{y} is originated from the parameter x which can be tuned from 0 to 0.5 by changing the frequency detuning Δ_s . In Fig. 4(b), we show kn as a function of z for $x = 0$, corresponding to the threshold value $\tilde{y} = 0$, and three different values of y as before. Under this condition, we find that the optical bistability phenomenon can be observed with the increase of z for arbitrary value of y with $y > 0$.

The second important externally controllable parameter, which can be used to control the bistability behavior, is y when x is given. In Fig. 4(c) we plot the normalized mean-photon number kn as a function of detuning y for $x = 0.5$, corresponding to the threshold value $\tilde{z} = 1/6\sqrt{3}$, and three different values $z_1 = 0.09 < 1/6\sqrt{3} = \tilde{z}$, $z_2 = 0.2 > 1/6\sqrt{3}$, and $z_3 = 0.3 > 1/6\sqrt{3}$, respectively. Fig. 4(c) shows that the optical bistability phenomenon cannot be observed for $z < \tilde{z}$ in contrast to the case $z > \tilde{z}$. Eq. (30) and Eq. (31) show that the threshold value \tilde{z} is proportional to the detuning parameter x . This means that the threshold value \tilde{z} can be reduced to zero when

$x = 0$. In Fig. 4(d), the normalized photon number kn is plotted as a function of y for $x = 0$, corresponding to the threshold value $\tilde{z} = 0$ of z , and three different parameters z_1 , z_2 and z_3 of the parameter z . Fig. 4(d) shows that the optical bistability phenomenon can be observed with the increase of y for arbitrary value of z with $z > 0$.

We now study how the parameter x affects the bistability. In Fig. 4(e), we plot kn as a function of z for $y = 0.8$ and three different parameters $x_1 = 0$, $x_2 = 0.25$ and $x_3 = 0.5$. The parameter $x_1 = 0$ corresponds to the zero threshold value for the parameters y and z . The parameter $x_2 = 0.25$ corresponds to the threshold values $\tilde{y} = x_2\sqrt{3}$ and $\tilde{z} = 4\tilde{y}^3/27$ for the parameters y and z respectively. However, the parameter $x_3 = 0.5$ corresponds to the maximum threshold values of the parameter y and z . It is clear that $y = 0.8$ is larger than the threshold values $\tilde{y} = 0$ corresponding to x_1 and $\tilde{y} = 0.433$ corresponding to x_2 , but $y = 0.8$ is below the threshold value $\tilde{y} = 0.87$ corresponding to x_3 . Thus, Fig. 4(e) clearly shows that kn as a function of z exhibits bistable behavior for the parameters x_1 and x_2 , but bistable behavior cannot be found for the given parameter x_3 . In Fig. 4(f) we show kn as a function of y for given parameter $z = 0.09$ and three same values $x_1 = 0$, $x_2 = 0.25$ and $x_3 = 0.5$ of the parameter x as in Fig. 4(e). Similar to Fig. 4(e), we find that kn curve exhibits bistable behavior for x_1 , corresponding to $\tilde{z} = 0$, and x_2 , corresponding to $\tilde{z} = 0.012$. However, we cannot find bistable behavior for kn curve with the parameter x_3 corresponding to $\tilde{z} = 0.096$.

According to above discussions, we can conclude that the nonlinear behavior in the optomechanical system can be transferred to the linear cavity resonator and controlled by using coherent feedback loop. The controlled bistability phenomena can be realized by adjusting the power and the frequency of externally applied driving field. In contrast to the bistability of optomechanical system [67] and by comparing Fig. 4(a) with Fig. 4(b), or comparing Fig. 4(c) with Fig. 4(d), we find that the threshold value of the bistable behavior can be reduced to zero even in the optomechanical system when the coherent feedback control is introduced.

V. COHERENT FEEDBACK INDUCED PHOTON BLOCKADE

We now turn to consider the case that the external driving field is weak enough and both cavity fields are in the quantum regime. We will study the single-photon blockade effect in the linear cavity induced by the coherent feedback control using an optomechanical system as a controller. The evolution of the coherent-feedback controlled system, comprised of the linear cavity and the optomechanical system, is described by the Hamiltonian of Eq. (11). In the rotating reference frame at the frequency ω_d of the driving field and under the Born-Markov approximation, the time evolution of the whole system is

described by a Lindblad-type master equation [94, 95]

$$\frac{d\rho}{dt} = \mathcal{L}(\rho) = -i[\tilde{H}, \rho] + \frac{1}{2}(2\tilde{L}\rho\tilde{L}^\dagger - \tilde{L}^\dagger\tilde{L}\rho - \rho\tilde{L}^\dagger\tilde{L}) + \gamma_m\mathcal{D}(b), \quad (33)$$

with

$$\tilde{L} = (\sqrt{\kappa} + \sqrt{\kappa_f})a + \sqrt{\gamma}c, \quad (34)$$

$$\mathcal{D}(b) = b\rho b^\dagger - \frac{1}{2}\rho b^\dagger b - \frac{1}{2}b^\dagger b\rho. \quad (35)$$

Here, we assume that the mechanical resonator and the cavity fields are in the zero-temperature environment for the convenience of calculations. The steady-state density operator ρ_{ss} can be obtained by setting $d\rho/dt = \mathcal{L}(\rho) = 0$, and then the normalized equal-time second-order correlation functions for both cavity fields in the steady-state case can be calculated by

$$g_a^{(2)}(0) = \frac{\langle a^\dagger a^\dagger aa \rangle}{\langle a^\dagger a \rangle^2} = \frac{\text{Tr}(\rho_{ss} a^\dagger a^\dagger aa)}{[\text{Tr}(\rho_{ss} a^\dagger a)]^2}, \quad (36)$$

$$g_c^{(2)}(0) = \frac{\langle c^\dagger c^\dagger cc \rangle}{\langle c^\dagger c \rangle^2} = \frac{\text{Tr}(\rho_{ss} c^\dagger c^\dagger cc)}{[\text{Tr}(\rho_{ss} c^\dagger c)]^2}. \quad (37)$$

Here, the subscripts a and c denote the cavity fields inside the controlled cavity and the cavity of the optomechanical system. Below, we will study the single-photon blockade effect in the linear cavity using Eq. (36). The single-photon blockade effect in the cavity of the optomechanical system can also be studied in a similar way.

A. Photon blockade in optomechanical single-photon strong-coupling regime

We now consider the statistical properties of photons when the optomechanical system is assumed to be in single-photon strong-coupling regime. For comparison, the second-order correlation functions $g_a^{(2)}(0)$ calculated by master equation and analytical solution are shown in Fig. 5. To analytically give the condition for photon blockade in the controlled cavity, the solution of $g_a^{(2)}(0)$ is obtained by the following method. With definition of the Kerr nonlinear coefficient $\chi = g_0^2/\omega_m$, in the rotating reference frame at the frequency ω_d of the driving field and under the condition $g_0/\omega_m \ll 1$, the effective Hamiltonian in Eq. (11) can be written as

$$\begin{aligned} \tilde{H}_{\text{eff}} = & \Delta_s a^\dagger a + (\Delta_c - \chi) c^\dagger c - \chi c^\dagger c c^\dagger c + \epsilon(c^\dagger + c) \\ & + \frac{i}{2}(\sqrt{\gamma\kappa} - \sqrt{\gamma\kappa_f})(a^\dagger c - c^\dagger a) + \omega_m b^\dagger b. \end{aligned} \quad (38)$$

Eq. (38) shows that the mechanical mode can be decoupled from the optical modes when all terms of parameter g_0/ω_m are neglected, thus let us assume that the state of the whole system is $|\psi\rangle = |\varphi\rangle|\phi\rangle_m$ where $|\varphi\rangle$ denotes the photon states of both cavity fields and $|\phi\rangle_m$

denotes the phonon states. Under the weak-driving condition, i.e. $\epsilon/\gamma \rightarrow 0$, we can describe the photon states as

$$|\varphi\rangle = \sum_{n_a=0}^2 \sum_{n_c=0}^2 C_{n_a, n_c} |n_a, n_c\rangle, \quad (39)$$

where $|n_a\rangle$ and $|n_c\rangle$ are the photon states of the controlled cavity and the cavity of optomechanical controller, respectively. It is obvious that $C_{00} \gg C_{01}, C_{10} \gg C_{11}, C_{20}, C_{02}$ under the weak driving condition $\epsilon/\gamma \rightarrow 0$. From Eq. (36), we can find

$$g_a^{(2)}(0) = \frac{\text{Tr}(\rho_{ss} a^\dagger a^\dagger a a)}{[\text{Tr}(\rho_{ss} a^\dagger a)]^2} = \frac{\sum_{n_a} n_a(n_a - 1) P_{n_a}}{[\sum_{n_a} n_a P_{n_a}]^2}. \quad (40)$$

in the steady-state. Here, P_{n_a} represents the probability of n_a photons distribution which can be expressed as

$$P_{n_a} = \sum_{n_c} |C_{n_a, n_c}|^2. \quad (41)$$

which means $P_{n_a} \gg P_{n_a+1}$ for $n_a \geq 2$.

To obtain the steady-state solution, we phenomenologically introduce the non-Hermitian complex Hamiltonian by setting the parameters as

$$\Delta_s \rightarrow \Delta_s - i(\sqrt{\kappa} + \sqrt{\kappa_f})^2/2, \quad (42)$$

$$\Delta_c \rightarrow \Delta_c - i\gamma/2. \quad (43)$$

in the Hamiltonian (38). Thus, under weak driving limit that the probabilities for more than three photon can be neglected, the second-order correlation function $g_a^{(2)}(0)$ can be expressed as [80]

$$g_a^{(2)}(0) = \frac{|\Delta_s + \Delta_c - 2\chi - i\kappa_a/2|^2 |\Delta_c - \chi - i\gamma/2|^2}{|(\Delta_s + \Delta_c - \chi - i\kappa_a/2)(\Delta_c - 2\chi - i\gamma/2)|^2}. \quad (44)$$

with

$$\kappa_a = (\sqrt{\kappa} + \sqrt{\kappa_f})^2 + \gamma. \quad (45)$$

Without loss of generality, we consider $\Delta_s = \Delta_c = \Delta$ which means that the controller cavity and the controlled cavity resonator are resonate with each other, thus the analytical solution of $g_a^{(2)}(0)$ is simplified to

$$g_a^{(2)}(0) = \frac{[4(\Delta - \chi)^2 + \kappa_a^2/4][(\Delta - \chi)^2 + \gamma^2/4]}{[(2\Delta - \chi - i\kappa_a/2)(\Delta - 2\chi - i\gamma/2)]^2}. \quad (46)$$

From Eq. (46) we can find that when the decay rates γ and κ_a are far less than the cavity detuning frequency Δ and the Kerr nonlinear coefficient χ , the second-order correlation function $g_a^{(2)}(0)$ becomes far less than one at the point of $\Delta/\chi = 1$. This means that the photon blockade occurs. In the following, we numerically study two

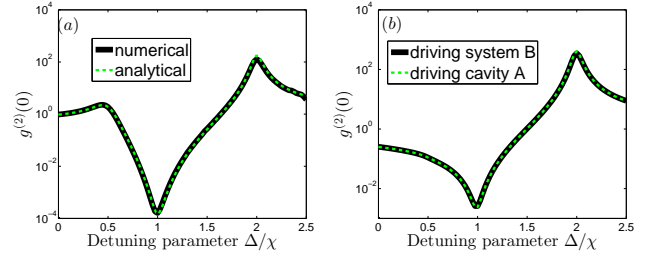


FIG. 5: Color online) The numerical and analytical solutions for second-order correlation function $g_a^{(2)}(0)$ of linear cavity field versus detuning parameter Δ/χ are shown in (a). The second-order correlation functions $g_c^{(2)}(0)$ of optomechanical cavity field versus detuning parameter Δ/χ by driving controlled cavity or controller cavity are shown in (b). The system parameters for this simulation are: $\kappa = \gamma$, $\kappa_f = \gamma$, $g_0 = 32\gamma$, $\omega_m = 100\gamma$, $\gamma_m = 0.01\gamma$, $\epsilon = 0.1\gamma$, $\gamma/2\pi = 1$ MHz.

very different parameter regions: (i) $\kappa = \kappa_f = \gamma$ and $g \sim \omega_m$ which are not easy to be achieved for current experiments; (ii) $\kappa = \kappa_f \gg \gamma$ and $g \ll \omega_m$ which are possible experimentally.

The second-order correlation function $g_a^{(2)}(0)$, calculated by master equation and analytical solution, as a function of Δ/χ is shown in Fig. 5(a) for $\kappa = \kappa_f = \gamma$ and $g_0 \sim \omega_m/3$. We find that the results obtained by numerical calculations and approximated solutions are almost same. Figure 5(a) shows that there is a minimum value at $\Delta/\chi = 1$ with $g_a^{(2)}(0) \ll 1$, which means that the photon blockade occurs and the single-photon can come out of the controlled cavity one by one. Figure 5(a) also shows that there is a maximum value at $\Delta/\chi = 2$ with $g_a^{(2)}(0) \gg 1$, which means that the two-photon tunneling occurs and photons can come out of the controlled cavity in pairs. These characteristics have been shown [70–72] in the standard optomechanical systems. However, the strong photon blockade and two-photon tunneling studied here are found in the controlled linear cavity, which is due to the coherent-feedback through the nonlinear quantum controller. This can be verified through $g_c^{(2)}(0)$, shown in Fig. 5(b), of the cavity field of the optomechanical system. We find a minimum value at $\Delta/\chi = 1$ corresponding to $g_c^{(2)}(0) \ll 1$ and a maximum value at $\Delta/\chi = 2$ corresponding to $g_c^{(2)}(0) \gg 1$. Thus, we would like to say that the photon blockade in the controller cavity is transferred to the controlled cavity by the coherent feedback loop. To answer the question whether the different driving strategy, such as driving the controlled cavity in contrast to driving controller cavity, can result in different optical nonlinear behavior, $g_c^{(2)}(0)$ for driving the controlled cavity is numerically studied and shown in Fig. 5(b), we find that there is no significant difference under these two different driving ways by given other parameters.

Let us now study another parameter regions, e.g., $\kappa = \kappa_f = 10\gamma$ and $g_0 = \omega_m/40$. The second-order corre-

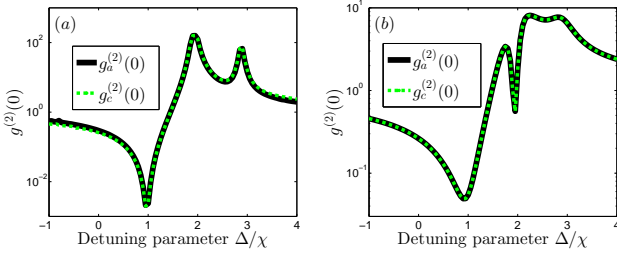


FIG. 6: (Color online) The second-order correlation functions $g_a^{(2)}(0)$ of controlled cavity field and $g_c^{(2)}(0)$ of optomechanical cavity field versus detuning parameter Δ/χ by driving the controlled cavity in (a) or driving the controller cavity in (b). The system parameters for this simulation are: $\kappa = 10\gamma$, $\kappa_f = 10\gamma$, $g_0 = 2.5\gamma$, $\omega_m = 100\gamma$, $\gamma_m = 0.01\gamma$, $\epsilon = 0.01\gamma$, $\gamma/2\pi = 1$ MHz.

lation functions of controlled cavity field and controller cavity field versus Δ/χ by driving the controlled cavity are shown in Fig. 6(a). We find that there exists a local minimum at $\Delta/\chi = 1$, a local maximum at $\Delta/\chi = 2$ and another local maximum at $\Delta/\chi = 3$ for each curve. The minimum value corresponding to $g_a^{(2)}(0) \ll 1$ and $g_c^{(2)}(0) \ll 1$ means that the photons in the controlled cavity and controller cavity can be blocked. The first local maximum at $\Delta/\chi = 2$ corresponding to $g_a^{(2)}(0) \gg 1$ and $g_c^{(2)}(0) \gg 1$ means that the single-photon transition from ground state to the first excited state is suppressed and second photon can enter the driven cavity making resonant transition from ground state to second excited state with the first photon. The second local maximum value at $\Delta/\chi = 3$ corresponding to $g_a^{(2)}(0) \gg 1$ and $g_c^{(2)}(0) \gg 1$ means that the three-photon resonant excitation happens and three-photon tunneling can be observed.

The second-order correlation functions of controlled cavity field and controller cavity field versus Δ/χ by driving the controller cavity are shown in Fig. 6(b). In contrast to the case that the controlled cavity is driven, we find that there exist a global minimum point at $\Delta/\chi = 1$, a local minimum at $\Delta/\chi = 2$ and local maximum at $\Delta/\chi = 3$ for each curve. The global minimum corresponding to $g_a^{(2)}(0) \ll 1$ and $g_c^{(2)}(0) \ll 1$ means that the photons in controlled cavity and controller cavity can be blocked. The local minimum at $\Delta/\chi = 2$ corresponding to $g_a^{(2)}(0) < 1$ and $g_c^{(2)}(0) < 1$ means that the two-photon tunneling is suppressed and photon blockade happens. The local maximum at $\Delta/\chi = 3$ corresponding to $g_a^{(2)}(0) \gg 1$ and $g_c^{(2)}(0) \gg 1$ means that the three-photon tunneling can be observed.

Comparing Fig. 6(a) with Fig. 6(b), and also in contrast to Fig. 5, we find that the second-order correlation functions present different behaviors for the different driving strategies in the region around the point $\Delta/\chi = 2$ under the condition $\kappa = \kappa_a \gg \gamma$. This difference comes from the unbalanced input-output rates of controlled cavity and controller cavity. When the driving field is ap-

plied to the controlled cavity and under the two-photon resonant driving ($\Delta/\chi = 2$), due to the output rate κ is much larger than the input rate γ , the first photon in controlled cavity transports to the controller cavity rapidly. Simultaneously, due to the output rates γ is much less than the input rates κ_f , the second photon has entered into the the controlled cavity before the first photon comes back. Therefore, at last the two-photon tunneling can be observed when the second photon meets the first one. However, When the driving field is applied to the controller cavity and under the two-photon resonant driving ($\Delta/\chi = 2$), due to the output rate γ is much less than the input rate κ_f , the first photon entering controller cavity cannot be transported to controlled cavity before the second photon is coming. Cooperated with the optomechanical nonlinearity, the first photon in the controller cavity prevents the second one from entering cavity and then the photon blockade occurs.

Comparing Fig. 5 with Fig. 6, we would like to mention that single-photon blockade can be more easily observed when the coherent-coupling strength $\sqrt{\kappa\gamma}$ and $\sqrt{\kappa_f\gamma}$ are enhanced no matter the driving is applied to controlled cavity or controller cavity. This is equivalent to enhance the coupling strength between two cavities for controlled system and optomechanical controller [77].

B. Photon blockade in optomechanical single-photon weak-coupling regime

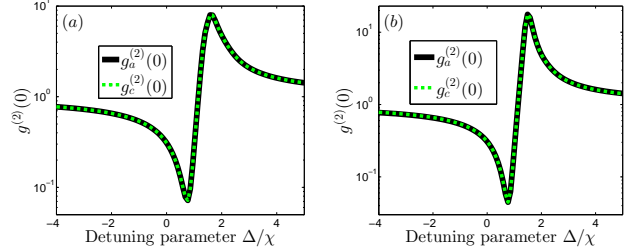


FIG. 7: (Color online) The second-order correlation functions $g_a^{(2)}(0)$ of linear cavity resonator and $g_c^{(2)}(0)$ of optomechanical controller versus detuning parameter Δ/χ by driving the optomechanical controller in (a) or driving the controller cavity in (b). The system parameters for this simulation are: $\kappa = \gamma$, $\kappa_f = 1.2\gamma$, $g_0 = 0.3\gamma$, $\omega_m = 10\gamma$. The other parameters are the same as in Fig. 6.

Let us now study the possibility on the photon blockade using coherent feedback control strategy in a weak single-photon optomechanical coupling regime, e.g., $g_0 = 0.3\gamma$. We focus on the statistical properties of photons. The second-order correlation function of controlled cavity field and controller cavity field versus Δ/χ are studied when the driving field is applied to the controller cavity.

As shown in Fig. 7(a), we can find that there exists a minimum near the point $\Delta/\chi = 1$ corresponding to $g_a^{(2)}(0) \ll 1$ and a maximum near the point $\Delta/\chi = 2$

corresponding to $g_a^{(2)}(0) \gg 1$. This means that the photons in controlled cavity can exhibit strong blockade and two-photon tunneling when it is coherently feedback controlled by an optomechanical controller even in weak optomechanical coupling. Fig. 7(a) also clearly shows that the curve of $g_a^{(2)}(0)$ fits well with the curve of $g_c^{(2)}(0)$ as well as which has been shown in Fig. 6. This is easily understood, because the controller cavity and the controlled cavity are coherently coupled with each other through the closed feedback loop with explicit photon flow direction, which is naturally determined by the propagation of the quantum field. Thus, if photon blockade (tunneling) occurs in the controller cavity, then the photons from the controller cavity are output one by one (two by two), and enter the controlled cavity, and vice versa.

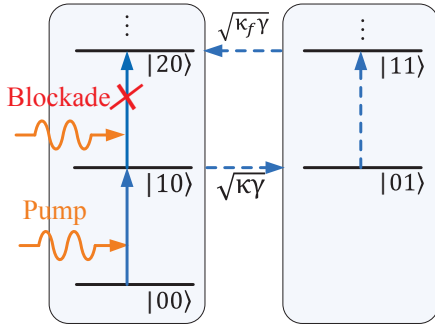


FIG. 8: (Color online) Schematic diagrams for two-photon exciting process. Two different transition paths leading to the destructive quantum interference which is responsible for the strong photon blockade. One path is the direct excitation from $|10\rangle$ to $|20\rangle$ and the other is drawn by the dotted arrows.

Similar to Fig. 7(a), the second correlation functions $g_a^{(2)}(0)$ and $g_c^{(2)}(0)$ versus Δ/χ are shown in Fig. 7(b) when the driving field is applied to the controlled cavity. Similar to the case for driving the controller cavity, a minimum near the point $\Delta/\chi = 1$ corresponding to $g_a^{(2)}(0), g_c^{(2)}(0) \ll 1$ and a maximum near the point $\Delta/\chi = 2$ corresponding to $g_a^{(2)}(0), g_c^{(2)}(0) \gg 1$ can be found. The only difference is that the minimum (maximum) value for driving controlled cavity is smaller (bigger) than that for driving controller cavity. That is, the photon blockade (tunneling) is better in driving controlled cavity than that for driving the controller cavity with the same parameters. We would also like to mention that single-photon blockade can be more easily observed when coherent-coupling strength g_0 is enhanced no matter the driving is applied to controlled cavity or controller cavity.

The strong photon blockade under weak optomechanical coupling comes from the cooperation between the weak Kerr nonlinearity in controller cavity induced by optomechanical interaction and the destructive interference for different paths of two-photon excitation process [96, 97]. In order to better understand the interference process, two different paths for two-photon ex-

citations are shown in Fig. 8. The first path is direct excitation from one photon to two photons in the driven cavity ($|00\rangle \rightarrow |20\rangle$). The second path is one photon coherently passed to the other one and finally comes back to the driven cavity ($|00\rangle \rightarrow |10\rangle \rightarrow |01\rangle \rightarrow |11\rangle \rightarrow |20\rangle$) which is unidirectional and uniquely determined by the propagation direction of quantum field. $\sqrt{\kappa_f\gamma}$ and $\sqrt{\kappa_f\gamma}$ can be considered as effective coupling strength between these two cavities, which is the key to induce destructive interference. It is obviously that the cavities' losses play a crucial role for achieving such destructive interference in contrast to other photon blockade systems introduced so far in which the cavities' losses always play a negative role.

We finally emphasize that the destructive interference due to the coherent feedback control is unidirectional determined by the propagation direction of the quantum field which is easier to be realized and controlled in contrast to that due to a cavity directly coupled to an optomechanical system [96, 97]. The cavity directly coupled scheme requires both individual addressability of each cavity and large coupling strength between each other through spatial proximity which is still a huge challenge [78]. However, in our proposed scheme, such two cavities are spatially separated by each other and directly coupling is replaced by coherent-feedback control which liberates such two cavities in space and eliminates the slashing requirement about challenging individual addressability and large coupling strength. Different from the single driving way by applying the driving field to the linear cavity in coupled-cavities scheme, our scheme can support another driving way, e.g., driving the controller cavity, which can also present strong photon blockade effect even in the optomechanical single-photon weak-coupling regime. Another significant difference is that both the controlled linear cavity and optomechanical controller cavity can emerge photon blockade simultaneously in contrast to the situation that only the linear cavity can emerge photon blockade and optomechanical system can not in coupled-cavity scheme.

VI. CONCLUSION

In summary, we have studied a system in which a linear cavity is coherently controlled by an optomechanical system through a closed feedback loop. The linear dynamics of the controlled cavity is nonlinearized by the optomechanical controller via the so-called feedback nonlinearization. The nonlinear controller using optomechanical systems and the coherent-feedback loop are the core of this strategy. Such coherent-feedback strategy can both liberates the controlled cavity and the optomechanical system in space and eliminates the slashing requirement about individual addressability or large coupling strength to achieve strong photon blockade in optomechanical weak-coupling regime. Moreover, we find that the coherent feedback control induced nonlinearity can

be used to demonstrate some other interesting nonlinear optical phenomena.

In the semiclassical regime, we found that optical bistability phenomenon in the controller cavity induced by the optomechanical interaction can be transferred to the controlled linear cavity through coherent feedback control. In particular, we found that the threshold value of the bistability can be significantly suppressed to zero through the coherent feedback control in contrast to finite threshold value of the bistability in pure optomechanical systems [67].

In the quantum regime, we study the statistical properties of photons of the controller cavity field and the controlled cavity field with two different driving strategies. We found that photon blockade both in the controller cavity and the controlled cavity is very similar under such two different driving methods when the output damping rates of the controlled cavity is comparable to those of the controller cavity. However, this similar effect can be broken when the output damping rates of the controlled cavity are much bigger than those of the controller cavity. Particularly, quite opposite quantum nonlinear behaviors, e.g., tunneling and blockade, are discussed in the region around the point $\Delta/\chi = 2$. Photon blockade can be observed when the coherent-coupling strengths $\sqrt{\kappa_f\gamma}$ and $\sqrt{\kappa_f\gamma}$ are enhanced no matter the driving is applied to controlled cavity or the controller cavity. Moreover, photon blockade can still happen even in the weak optomechanical coupling regime due to the destructive quantum interference induced by coherent feedback control. It is

worth noting that the cavities's losses are actually crucial for achieving photon blockade in such coherent-feedback approach in contrast to photon blockade systems introduced so far in which the cavities' losses always play a negative role.

We hope that our study can provide a controllable way to engineer strong quantum nonlinearity, such as the control of photon transmission through a linear cavity by using a optomechanical controller, achieving strong photon blockade under weak optomechanical coupling condition and serving as single-photon devices. We also hope that such proposed design can have potential applications in quantum state engineering, quantum computing and quantum communication.

VII. ACKNOWLEDGEMENT

Y.X.L. is supported by the National Natural Science Foundation of China under Grant Nos. 61025022, 61328502, 91321208. J.Z. is supported by the National Natural Science Foundation of China under Grant Nos. 61174084, 61134008. Y.X.L. and J.Z. are supported by the National Basic Research Program of China 973 Program under Grant No. 2014CB921401, the Tsinghua University Initiative Scientific Research Program, and the Tsinghua National Laboratory for Information Science and Technology (TNList) Cross-discipline Foundation.

-
- [1] T. A. Fulton and G. J. Dolan, Phys. Rev. Lett. **59**, 109 (1987).
 - [2] M. A. Kastner, Reviews of Modern Physics **64**, 849 (1992).
 - [3] K. K. Likharev, Proc. IEEE **87**, 606 (1999).
 - [4] A. Imamoglu, H. Schmidt, G. Woods, and M. Deutsch, Phys. Rev. Lett. **79**, 1467 (1997).
 - [5] P. Grangier, D. F. Walls, and K. M. Gheri, Comment on "Strong interacting photons in a nonlinear cavity", Phys. Rev. Lett. **81**, 2833 (1998).
 - [6] F.-Y. Hong and S.-J. Xiong, Phys. Rev. A **78**, 013812 (2008).
 - [7] B. Dayan, A. S. Parkins, T. Aoki, E. P. Ostby, K. J. Vahala, and H. J. Kimble, Science **319**, 1062 (2008).
 - [8] T. Aoki, A. S. Parkins, D. J. Alton, C. A. Regal, B. Dayan, E. Ostby, K. J. Vahala, and H. J. Kimble, Phys. Rev. Lett. **102**, 083601 (2009).
 - [9] P. Michler, A. Kiraz, C. Becher, W. V. Schoenfeld, P. M. Petroff, L. Zhang, E. Hu, and A. Imamoglu, Science **290**, 2282 (2000).
 - [10] L. Zhou, L. P. Yang, Y. Li, and C. P. Sun, Phys. Rev. Lett. **111**, 103604 (2013).
 - [11] S. Rosenblum, S. Parkins, and B. Dayan, Phys. Rev. A **84**, 033854 (2011).
 - [12] A. Faraon, I. Fushman, D. Englund, N. Stoltz, P. Petroff, and J. Vučković, Nat. Phys. **4**, 859 (2008).
 - [13] Q. A. Turchette, C. J. Hood, W. Lange, H. Mabuchi, and H. J. Kimble, Phys. Rev. Lett. **75**, 25 (1995).
 - [14] D. Schrader, I. Dotsenko, M. Khudaverdyan, Y. Miroshnychenko, A. Rauschenbeutel, and D. Meschede, Phys. Rev. Lett. **93**, 150501 (2004).
 - [15] G. J. Milburn, Phys. Rev. Lett. **62**, 18 (1989).
 - [16] H. M. Gibbs, *Optical Bistability: Controlling Light with Light* (Academic, Orlando, 1985).
 - [17] J. L. O'Brien, Science **318**, 1567 (2007).
 - [18] K. M. Birnbaum, A. Boca, R. Miller, A. D. Boozer, T. E. Northup, and H. J. Kimble, Nature **436**, 87 (2005).
 - [19] D. Englund, A. Majumdar, A. Faraon, M. Toishi, N. Stoltz, P. Petroff, and J. Vučković, Phys. Rev. Lett. **104**, 073904 (2010).
 - [20] C. Lang, D. Bozyigit, C. Eichler, L. Steffen, J. M. Fink, A. A. Abdumalikov, M. Baur, S. Filipp, M. P. da Silva, A. Blais, and A. Wallraff, Phys. Rev. Lett. **106**, 243601 (2011).
 - [21] A. J. Hoffman, S. J. Srinivasan, S. Schmidt, L. Spietz, J. Aumentado, H. E. Tüci, and A. A. Houck, Phys. Rev. Lett. **107**, 053602 (2011).
 - [22] T. J. Kippenberg and K. J. Vahala, Science **321**, 1172 (2008).
 - [23] F. Marquardt and S. M. Girvin, Physics **2**, 40 (2009).
 - [24] A. A. Clerk, M. H. Devoret, S. M. Girvin, F. Marquardt, and R. J. Schoelkopf, Rev. Mod. Phys. **82**, 1155 (2010).

- [25] M. Aspelmeyer, P. Meystre, and K. Schwab, *Phys. Today* **65**, 29 (2012).
- [26] M. Aspelmeyer, T. J. Kippenberg, and F. Marquardt, arXiv:1303.0733.
- [27] V. B. Braginsky, S. E. Strigin, and S. P. Vyatchanin, *Phys. Lett. A* **305**, 111 (2002).
- [28] J. M. Courty, A. Heidmann, and M. Pinard, *Phys. Rev. Lett.* **90**, 083601 (2003).
- [29] T. Corbitt, Y. Chen, E. Innerhofer, H. Müller-Ebhardt, D. Ottaway, H. Rehbein, D. Sigg, S. Whitcomb, C. Wipf, and N. Mavalvala, *Phys. Rev. Lett.* **98**, 150802 (2007).
- [30] W. Marshall, C. Simon, R. Penrose, and D. Bouwmeester, *Phys. Rev. Lett.* **91**, 130401 (2003).
- [31] D. Rugar, R. Budakian, H. J. Mamin, and B. W. Chui, *Nature* **329** (2004).
- [32] P. Rabl, S. J. Kolkowitz, F. H. L. Koppens, J. G. E. Harris, P. Zoller, and M. D. Lukin, *Nat. Phys.* **6**, 602 (2010).
- [33] S. Gigan, H. R. Böhm, M. Paternostro, F. Blaser, G. Langer, J. B. Hertzberg, K. C. Schwab, D. Bäuerle, M. Aspelmeyer, and A. Zeilinger, *Nature* **444**, 67 (2006).
- [34] O. Arcizet, P.-F. Cohadon, T. Briant, M. Pinard, and A. Heidmann, *Nature* **444**, 71 (2006).
- [35] A. Schliesser, P. Del’Haye, N. Nooshi, K. Vahala, and T. Kippenberg, *Phys. Rev. Lett.* **97**, 243905 (2006).
- [36] I. Wilson-Rae, N. Nooshi, W. Zwerger, and T. J. Kippenberg, *Phys. Rev. Lett.* **99**, 093901 (2007).
- [37] F. Marquardt, J. Chen, A. Clerk, and S. Girvin, *Phys. Rev. Lett.* **99**, 093902 (2007).
- [38] J. Teufel, J. Harlow, C. Regal, and K. Lehnert, *Phys. Rev. Lett.* **101**, 197203 (2008).
- [39] J. D. Thompson, B. M. Zwickl, A. M. Jayich, F. Marquardt, S. M. Girvin, and J.G.E. Harris, *Nature* **452**, 72 (2008).
- [40] A. Schliesser, R. Rivière, G. Anetsberger, O. Arcizet, and T. J. Kippenberg, *Nat. Phys.* **4**, 415 (2008).
- [41] S. Gröblacher, J. B. Hertzberg, M. R. Vanner, G. D. Cole, S. Gigan, K. C. Schwab, and M. Aspelmeyer, *Nat. Phys.* **5**, 485 (2009).
- [42] T. Rocheleau, T. Ndukum, C. Macklin, J. B. Hertzberg, A. A. Clerk, and K. C. Schwab, *Nature* **463**, 72 (2010).
- [43] Y. S. Park and H. Wang, *Nat. Phys.* **5**, 489 (2009).
- [44] A. Schliesser, O. Arcizet, R. Rivière, G. Anetsberger, and T. J. Kippenberg, *Nat. Phys.* **5**, 509 (2009).
- [45] J. D. Teufel, T. Donner, D. Li, J. W. Harlow, M. S. Allman, K. Cicak, A. J. Sirois, J. D. Whittaker, K. W. Lehnert, and R. W. Simmonds, *Nature* **475**, 359 (2011).
- [46] J. Chan, T.P.M. Alegre, A. H. Safavi-Naeini, J. T. Hill, A. Krause, S. Gröblacher, M. Aspelmeyer, and O. Painter, *Nature* **478**, 89 (2011).
- [47] E. Verhagen, S. Deléglise, S. Weis, A. Schliesser, and T. J. Kippenberg, *Nature* **482**, 63 (2012).
- [48] T. Carmon, H. Rokhsari, L. Yang, T. J. Kippenberg, and K. J. Vahala, *Phys. Rev. Lett.* **94**, 223902 (2005).
- [49] T. J. Kippenberg, H. Rokhsari, T. Carmon, A. Scherer, and K. J. Vahala, *Phys. Rev. Lett.* **95**, 033901 (2005).
- [50] J. D. Teufel, D. Li, M. S. Allman, K. Cicak, A. J. Sirois, J. D. Whittaker, and R. W. Simmonds, *Nature* **471**, 204 (2011).
- [51] G. S. Agarwal and S. Huang, *Phys. Rev. A* **81**, 041803(R) (2010).
- [52] S. Huang and G. S. Agarwal, *Phys. Rev. A* **83**, 043826 (2011).
- [53] S. Weis, R. Rivière, S. Deléglise, E. Gavartin, O. Arcizet, A. Schliesser, and T. J. Kippenberg, *Science* **330**, 1520 (2010).
- [54] A. H. Safavi-Naeini, T. P. Mayer Alegre, J. Chan, M. Eichenfield, M. Winger, Q. Lin, J. T. Hill, D. E. Chang, and O. Painter, *Nature* **472**, 69 (2011).
- [55] D. Vitali, S. Gigan, A. Ferreira, H. R. Böhm, P. Tombesi, A. Guerreiro, V. Vedral, A. Zeilinger, and M. Aspelmeyer, *Phys. Rev. Lett.* **98**, 030405 (2007).
- [56] M. J. Hartmann and M. B. Plenio, *Phys. Rev. Lett.* **101**, 200503 (2008).
- [57] K. Stannigel, P. Rabl, A. S. Sørensen, P. Zoller, and M. D. Lukin, *Phys. Rev. Lett.* **105**, 220501 (2010).
- [58] S. Gröblacher, K. Hammerer, M. R. Vanner, and M. Aspelmeyer, *Nature* **460**, 724 (2009).
- [59] L. Tian and H. Wang, *Phys. Rev. A* **82**, 053806 (2010); L. Tian, *Phys. Rev. Lett.* **108**, 153604 (2012).
- [60] Y. D. Wang and A. A. Clerk, *Phys. Rev. Lett.* **108**, 153603 (2012).
- [61] S. A. McGee, D. Meiser, C. A. Regal, K. W. Lehnert, and M. J. Holland, *Phys. Rev. A* **87**, 053818 (2013).
- [62] J. T. Hill, A. H. Safavi-Naeini, J. Chan, and O. Painter, *Nat. Commun.* **3**, 1196 (2012).
- [63] C. Dong, V. Fiore, M. C. Kuzyk, and H. Wang, *Science* **338**, 1609 (2012).
- [64] J. Bochmann, A. Vainsencher, D. D. Awschalom, and A. N. Cleland, *Nat. Phys.* **9**, 712 (2013).
- [65] R. W. Andrews, R. W. Peterson, T. P. Purdy, K. Cicak, R. W. Simmonds, C. A. Regal, and K. W. Lehnert, *Nature Phys.* **10**, 321 (2014).
- [66] Z. R. Gong, H. Ian, Y. X. Liu, C. P. Sun, and F. Nori, *Phys. Rev. A* **80**, 065801 (2009).
- [67] S. Aldana, C. Bruder, and A. Nunnenkamp, *Phys. Rev. A* **88**, 043826 (2013).
- [68] X. Y. Lü, W. M. Zhang, S. Ashhab, Y. Wu, and F. Nori, *Scientific Rep.* **3**, 2943 (2013).
- [69] G. S. Agarwal and S. Huang, *Phys. Rev. A* **85**, 021801(R) (2012).
- [70] P. Rabl, *Phys. Rev. Lett.* **107**, 063601 (2011).
- [71] A. Nunnenkamp, K. Børkje, and S. M. Girvin, *Phys. Rev. Lett.* **107**, 063602 (2011).
- [72] X. W. Xu, Y. J. Li, and Y. X. Liu, *Phys. Rev. A* **87**, 025803 (2013).
- [73] J. Q. Liao, H. K. Cheung, and C. K. Law, *Phys. Rev. A* **85**, 025803 (2012).
- [74] J. Q. Liao and F. Nori, *Phys. Rev. A* **88**, 023853 (2013).
- [75] K. Stannigel, P. Komar, S. J. M. Habraken, S. D. Bennett, M. D. Lukin, P. Zoller, and P. Rabl, *Phys. Rev. Lett.* **109**, 013603 (2012).
- [76] M. Ludwig, A. H. Safavi-Naeini, O. Painter, and F. Marquardt, *Phys. Rev. Lett.* **109**, 063601 (2012).
- [77] X. W. Xu and Y. J. Li, *J. Opt. B: At. Mol. Opt. Phys.* **46**, 035502 (2013).
- [78] A. Majumdar, M. Bajcsy, A. Rundquist and J. Vučković, *Phys. Rev. Lett.* **108**, 183601 (2012).
- [79] J. Zhang, R. B. Wu, Y. X. Liu, and C. W. Li, *IEEE Trans. Automat. Contr.* **57**, 1997 (2012).
- [80] Z. P. Liu, H. Wang, J. Zhang, Y. X. Liu, R. B. Wu, C. W. Li, and F. Nori, *Phys. Rev. A* **88**, 063851 (2013).
- [81] H. Wiseman and G. Milburn, *Physical Review A* **49**, 4110 (1994).
- [82] S. Lloyd, *Phys. Rev. A* **62**, 022108 (2000); R. J. Nelson, Y. Weinstein, D. Cory, and S. Lloyd, *Phys. Rev. Lett.* **85**, 3045 (2000).
- [83] H. Mabuchi, *Phys. Rev. A* **78**, 032323 (2008); M. Armen,

- J. Au, J. Stockton, A. Doherty, and H. Mabuchi, Phys. Rev. Lett. **89**, 133602 (2002).
- [84] G. G. Gillett, R. B. Dalton, B. P. Lanyon, M. P. Almeida, M. Barbieri, G. J. Pryde, J. L. O'Brien, K. J. Resch, S. D. Bartlett, and A. G. White, Phys. Rev. Lett. **104**, 080503 (2010).
- [85] M. R. James, H. I. Nurdin, and I. R. Petersen, IEEE Trans. Automat. Contr. **53**, 1787 (2008).
- [86] J. Gough and M. R. James, IEEE Trans. Automat. Contr. **54**, 2530 (2009).
- [87] M. Yanagisawa and H. Kimura, IEEE Trans. Automat. Contr. **48**, 2107 (2003).
- [88] Z. Zhou, C. Liu, Y. Fang, J. Zhou, R. T. Glasser, L. Chen, J. Jing, and W. Zhang, Appl. Phys. Lett. **101**, 191113 (2012).
- [89] J. Kerckhoff and K. W. Lehnert, Phys. Rev. Lett. **109**, 153602 (2012).
- [90] A. Kubanek, M. Koch, C. Sames, A. Ourjoumtsev, P. W. H. Pinkse, K. Murr, and G. Rempe, Nature **462**, 898 (2009).
- [91] H. Yonezawa, D. Nakane, T. A. Wheatley, K. Iwasawa, S. Takeda, H. Arao, K. Ohki, K. Tsumura, D. W. Berry, T. C. Ralph, H. M. Wiseman, E. H. Huntington, and A. Furusawa, Science **337**, 1514 (2012).
- [92] O. Arcizet, P.-F. Cohadon, T. Briant, M. Pinard, and A. Heidmann, Nature **444**, 71 (2006); D. Kleckner and D. Bouwmeester, Nature **444**, 75 (2006).
- [93] J. Zhang, Y. X. Liu, R. B. Wu, K. Jacobs, and F. Nori, Phys. Rev. A **87**, 032117 (2013).
- [94] D. F. Walls and G. J. Milburn, *Quantum Optics* (Springer-Verlag, Heidelberg, 2008).
- [95] R. R. Puri, Mathematical Methods of Quantum Optics (Springer-Verlag, Berlin, 2001).
- [96] M. Bamba, A. Imamoglu, I. Carusotto, and C. Ciuti, Phys. Rev. A **83**, 021802 (2011).
- [97] T.C.H. Liew and V. Savona, Phys. Rev. Lett. **104**, 183601 (2010).